

Ain Shams University
Faculty of Science
Geophysics Department



MULTI-DIMENSIONAL FORWARD AND INVERSE MODELING OF THE HIGH-RESOLUTION AIRBORNE TOTAL MAGNETIC INTENSITY DATA AT WEST EDFU REGION, WESTERN DESERT - EGYPT

A Thesis

**Submitted in a Partial Fulfillment for the Requirements of M.Sc. Degree of Science in
Applied Geophysics**

BY

AHMAD HAMDI MUHAMMAD MUHAMMAD HABEEB

(B.Sc. in Geophysics, Ain Shams University, 2008)

To

**Geophysics Department,
Faculty of Science,
Ain Shams University**

Supervised by

Prof. Dr. Sami Hamed Abd El Nabi

Professor of Geophysics
Geophysics Department, Faculty of Science,
Ain Shams University.

Prof. Dr. Ali Mohamed Sabri Abdelaziz

Professor of Geophysics,
Head of Airborne Geophysics Department,
Nuclear Materials Authority.

Dr. Karam Samir Ibrahim Farag

Lecturer of Geophysics,
Ain Shams University,
Cairo-Egypt.

Cairo -2017

ACKNOWLEDGEMENTS

Praise is to ALLAH, the Lord of the worlds, by whose grace this work has been completed.

The author wishes to express his thanks and gratitude to Dr. / Sami Hamed Abd El Nabi

, Professor of applied geophysics, Geology Dept., Faculty of science, Ain-shams University, Cairo, Egypt, for his supervision, encouragement, valuable advice throughout the stages of the work and revising the manuscript.

The author is especially appreciative to Dr. Ali M. S. Abdelaziz, Professor of applied geophysics, and Vice Head of Airborne Geophysics Department, Exploration Division, Nuclear Materials Authority, Cairo, Egypt, for his continuous help and support, fruitful discussion and criticism as well as for his supervision of this study and his critical reviewing of the manuscript.

The author is deeply grateful to Dr. Alaa Eldin A. F. Aref, Professor of applied geophysics and Vice Head of Exploration Division, Nuclear Materials Authority, Cairo, Egypt, for his faithful guidance.

The author wishes to express his thanks and gratitude to Dr./ Karam Samir Farag , Lecturer of applied geophysics, Geology Dept., Faculty of science, Ain-shams University, Cairo, Egypt, for his supervision, encouragement, valuable advice throughout the stages of the work and revising the manuscript.

The author is deeply grateful to Dr. Atef Mahmoud Ismail, Professor of applied geophysics and Head of Airborne Geophysics Department, Cairo, Egypt, faithful guidance.

The author is deeply grateful to Dr. Abd El Mohsen Galal Nady Garieb, Professor of Applied Geophysics, Exploration Division Nuclear Materials Authority, NMA, Cairo, Egypt, for faithful guidance.

My sincere thanks to all members of airborne geophysics department especially my friends Sayed, Salwa, Enaam, Ali, Rehab, Sara, Essam, Emad, Osama Wadie, Ramadan, M. Abdelatif, Tamer, Osama Zaki, A. Gamal and A. Ramadan.

My grateful acknowledgement to my parents for their encouragement and their sincere help, my sisters (Rasha, Rehab and Dina).

Deep thanks are also directed to my friends Hassan, Islam Hussien, HaithamFathi and Remon Aziz.

A. HamdiHabeeb

ABSTRACT

West Edfu Area is located in the western Desert and stretches along the western blank of Lake Nasser and Nile River, which is bounded from the West by Sin El kaddab plateau covering an area of approximately 9800 km². The area is bounded from the west by bahariya oasis and from the south by Aswan Lake and from the East by Nile River and Edfu city.

The study area has been covered recently by systematic aerial magnetic and multi-channel gamma-ray survey. This survey was flown by the Airborne Geophysics Department, Exploration Division, Nuclear Materials Authority (NMA) of Egypt in October, 2011. This mission has accomplished using the NMA geophysical survey twin-engine Beechcraft king Air B200SE (Turbine engines) equipped with a multi - sensor airborne geophysical survey system. This comprises a high resolution Cesium vapor magnetometer. Communication instruments installed on the aircraft are Collins products. NMA Aircraft has the Egyptian registration No. SU-BNJ.

The airborne magnetic data obtained from the survey over West Edfu area has been analyzed by various techniques. These techniques include the reduction to the north magnetic pole (RTP), isolation of the regional and residual magnetic components using band pass filtering technique, calculation of the second vertical derivative, magnetic depth calculation and 2D and 3D magnetic modeling technique.

The integration of all these techniques has been resulted in the construction of the interpreted basement tectonic map for the present study area. The encountered deep-seated Precambrian basement structures are generally trending NW–SE and NE–SW directions. The depth-to-the-basement estimates were reliably varied between 130 and 4750 m, from the existing averaged ground surface, and correlated well with the available drilled stratigraphic-control wells. Additionally, the results suggested that the sedimentary cover is tectonically affected by such deep-seated basement structures with a set of tectonic faults extending from the basement upwards through the sedimentary cover. These faulted sedimentary blocks may constitute potential structural traps for the hydrocarbon accumulation.

CONTENTS

	Page
AKNOWLEDGEMENTS.....	I
ABSTRACT.....	II
CONTENTS.....	III
LIST OF FIGURES.....	VII
LIST OF TABLES.....	IX
<i>CHAPTER ONE</i>	
<i>INTRODUCTION</i>	1
1.1. GENERAL.....	1
1.2. LOCATION.....	4
1.3. CLIMATE AND VEGETATION.....	5
1.4. TOPOGRAPHY AND GEOMORPHOLOGY.....	6
1.5. PREVIOUS WORK.....	7
1.6. AIM AND SCOPE OF WORK.....	9

CHAPTER TWO	12
REGIONAL GEOLOGY OF WEST EDFU AREA	
2.1. GENERAL GEOLOGY.....	12
2.2. REGIONAL STRUCTURAL FRAMEWORK OF WEST EDFU AREA.....	13
2.3. STRATIGRAPHY OF WEST EDFU AREA.....	14
2.3.1. GRAVEL TRACES.....	16
2.3.2. SERAI FORMATION (=THEBES).....	16
2.3.3. EL RUFUF FORMATION.....	16
2.3.4. DUNGUL FORMATION	17
2.4. DEPOSITIONAL ENVIRONMENT.....	17
2.5. STRUCTURAL ELEMENTS.....	17
2.5.1. FAULTS.....	17
2.5.1.1. NW-SE TO NNW-SSE ORIENTED FAULTS.....	17
2.5.1.2. NE-SW TO NNE-SSW ORIENTED FAULTS.....	18
2.5.1.3.E-W ORIENTED FAULTS.....	18
2.5.1.4. N-S ORIENTED FAULTS.....	19
2.5.2. FOLDS	19
2.5.2.1. NNW-SSE ORIENTED FOLDS.....	19
2.5.2.2. NNE-SSW ORIENTED FOLDS.....	19
2.5.2.3. EE-WSW AND ESE-WNW ORIENTED FOLDS.....	19
2.5.2.4. NNE-SSW, ENE-WSW AND ESE-WNW ORIENTED FOLD.....	20
CHAPTER THREE	21
AIRBORNE GEOPHYSICAL SURVEY	
3.1. GENERAL.....	21
3.2. SURVEY GRID.....	22
3.3. AIRCRAFT AND GROUND EQUIPMENTS.....	22
3.3.1. AIRCRAFT.....	22
3.3.1.1. ELECTRONIC NAVIGATION	22
3.3.1.2. ALTIMETER.....	23
3.3.1.3.AIRBORNE MAGNETOMETER.....	23

3.3.2. BASE STATION MAGNETOMETER.....	24
3.3.3. DATA ACQUISITION / RECORDING SYSTEM.....	25
3.4. PRE-SURVEY CHECKS, TESTS AND CALIBRATION.....	26
3.4.1. AIRBORNE / GROUND MAGNETOMETER.....	27
3.4.2. FIGURE OF MERIT (FOM).....	27
3.4.3. NOISE TEST.....	28
3.4.4. HEADING TEST.....	28
3.4.5. PARALLAX / LAG TEST.....	29
3.4.6. BASE STATION MAGNETOMETER CHECK.....	29
3.4.7. NAVIGATION SYSTEM.....	29
3.4.7.1. GPS BASE STATION LOCATION.....	29
3.4.7.2. ALTIMETER CALIBRATION.....	30
3.5. AIRBORNE MAGNETOMETER NOISE LEVELS.....	30
3.5.1. DIURNAL VARIATION AND MICROPULSATIONS.....	31
3.6. NAVIGATION.....	31
3.6.1. GPS SYSTEM.....	31
3.6.2. LINE POSITIONING.....	32
3.6.3. FLIGHT ELEVATION / SPEED.....	32
3.7. AIRBORNE MAGNETIC PROCESSING.....	32
3.7.1. DIURNAL CORRECTION.....	33
3.7.2. SPIKE AND NOISE REJECTION.....	33
3.7.3. HEADING CORRECTION.....	33
3.7.4. PARALLAX / LAG CORRECTION.....	33
3.7.5. INTERNATIONAL GEOMAGNETIC REFERENCE FIELD (IGRF).....	34
3.7.6. LEVELING.....	34
3.7.6.1. THE PROBLEM.....	34
3.7.6.2. LEVELING TIE LINES.....	35
3.7.6.3. LEVELING SURVEY LINES.....	36
3.8. DATA PRESENTATION.....	36
3.8.1. GRIDDING OF THE GEOPHYSICAL DATA.....	36

3.8.2. CONVERSION OF AIRBORNE GEOPHYSICAL DATA TO IMAGE FORMAT.....	37
--	----

CHAPTER FOUR

MAGNETIC ANALYSIS AND INTERPRETATION

4.1. GENERAL.....	39
4.2. FREQUENCY-DOMAIN PROCESSING.....	41
4.3. REDUCTION TO THE NORTH MAGNETIC POLE.....	42
4.4. COMPUTATION AND ANALYSIS OF THE ENERGY (POWER) SPECTRUM.....	45
4.5. SEPERATION OF MAGNETIC ANOMALIES.....	46
4.5.1. GAUSSIAN REGIONAL / RESIDUAL FILTER.....	47
4.6. COMPUTATION OF THE SECOND VERTICAL DERIVATIVE (SVD).....	50
4.7. MAGNETIC DEPTH CALCULATION.....	51
4.7.1. ANALYTIC SIGNAL.....	51
4.7.2. SOURCE PARAMETER IMAGING (SPI).....	54
4.7.3. DEPTH ESTIMATION BY 3D EULER DECONVOLUTION.....	56
4.8. INTERPRETATION OF AIRBORNE MAGNETIC SURVEY DATA.....	60
4.8.1.GENERAL.....	60
4.8.2. QUALITATIVE INTERPRETATION OF AIRBORNE MAGNETIC SURVEY DATA.....	61
4.8.2.1. GENERAL.....	61
4.8.2.2. DESCRIPTION OF THE AERIAL MAGNETIC MAPS.....	62
4.8.3. QUANTITATIVE INTERPRETATION OF AIRBORNE MAGNETIC SURVEY DATA.....	63
4.8.3.1.GENERAL.....	63
4.8.3.2. DEPTH CALCULATION RESULTS.....	64
4.8.4. INTERPRETED MAGNETIC BASEMENTTECTONIC MAP.....	64

CHAPTER FIVE

FORWARD AND INVERSE MODELLING

67

5.1. INTRODUCTION.....	67
5.2. MAGNETIC FORWARD MODELLING.....	69
5.3. MAGNETIC INVERSE MODELLING	70
5.4. MAIN PROBLEMS OF INVERSION.....	70
5.4.1. EXISTENCE OF SOLUTION.....	72
5.4.2. EXISTENCE OF UNIQUE SOLUTION.....	72
5.4.3. EXISTENCE OF STABLE SOLUTION.....	72
5.5. INVERSION METHODS.....	73
5.5.1. LEAST SQUARE INVERSION.....	73
5.5.2. MINIMUM NORM INVERSION.....	74
5.5.3. MARQUARDT-LEVENBERG INVERSION.....	74
5.6. INTERACTIVE TWO DIMENTIONALMAGNETIC MODELING.....	76
5.7. THREE-DIMENTIONAL MAGNETIC MODELING INTERPRETATION.....	82
5.7.1. MAGNETIC SUSCEPTIBILITY	85
5.7.1.1. CONSTANT SUCEPTIBILITY.....	85
5.7.1.2. LATERAL SUSCEPTIBILITY DISTRIBUTION.....	88
5.7.2. ANALYSIS FOR INVERSION PROCESS.....	89
5.7.3. RECOMMENDATION FOR INVERSION WORK.....	90
5.7.4. DEPTH ESTIMATION TECHNIQUE ANDINVERSION PROCESS.....	90
SUMARRY AND CONCLUSION.....	92
REFRENCES.....	95

LIST OF FIGURES

Figure 1: Three categories of techniques to interpret potential field data. Measured anomaly is represented by a , calculated anomaly by A_o , and transformed measured anomaly by A' . Parameters p_1, p_2, \dots are attributes of the source, such as depth, thickness, density, or magnetization.

Figure 2: location map of West Edfu area Western Desert of Egypt.

Figure 3: Topographic Map of West Edfu area, Western Desert, Egypt.

Figure 4: Geologic Map of West Edfu Area, Western Desert, Egypt, (After Conco, 1987).

Figure 5: Beechcraft B200SE Geophysical Exploration Aircraft.

Figure 6: Screen Display for Airborne Geophysical Information System (AGIS).

Figure 7: Total magnetic intensity field map, West Edfu area, Western desert, Egypt.

Figure 8: Reduced to the north magnetic pole (RTP) map, West Edfu area, Western desert, Egypt.

Figure 9: Power spectrum of magnetic data showing the corresponding averaging depths, of West Edfu area, Western Desert, Egypt.

Figure 10: Typical Gaussian filter technique of separation after Reford and Summer (1964).

Figure 11: Regional magnetic field intensity component map, West Edfu area, Western desert, Egypt

Figure 12: Residual magnetic field intensity component map, West Edfu area, Western desert, Egypt.

Figure 13: Second vertical derivative in depth direction map, West Edfu area, Western desert,

Egypt

Figure 14: Depth to magnetic basement map calculated using Analytical signal method (AS), West Edfu area, Western desert, Egypt

Figure 15: Depth to magnetic basement map calculated using source parameter imaging method (SPI), West Edfu area, Western desert, Egypt

Figure 16: Standard Euler Depth solution of Structural Index $SI = 0.0$, depth uncertainty dz : 25%

Figure 17: Basement Tectonic map for West Edfu area, Western Desert, Egypt.

Figure 18: 2D profile location for profile A-A', B-B', C-C' and D-D' and the well location WKO-1X and WKO-3X.

Figure 19: The 2D inverted susceptibility layered-earth model and calculated geomagnetic response below the long RTP traverse A-A'. Location of the available drilled stratigraphic-control well 'WKO-3X', which was used wisely to constrain the interactive inversion results, is donated.

Figure 20: The 2D inverted susceptibility layered-earth model and calculated geomagnetic response below the long RTP traverse B-B'. Location of the available drilled stratigraphic-control well 'WKO-1X', which was used wisely to constrain the interactive inversion results, is donated.

Figure 21: The 2D inverted susceptibility layered-earth model and calculated geomagnetic response below the short RTP traverse C-C'

Figure 22: The 2D inverted susceptibility layered-earth model and calculated geomagnetic response below the long RTP traverse D-D'. Location of the available drilled stratigraphic-control well 'WKO-3X', which was used wisely to constrain the interactive inversion results, is donated.

Figure 23: Results of GMSYS-3D and including the flowing: a) observed regional magnetic, b) calculated magnetic, c) data misfit.

Figure 24: Inverted Depth to Basement Surface from 3D Magnetic Modelling using lateral susceptibility distribution.

Figure 25: Inverted Vs. actual depths at drilled well location WKO-1X and WKO-3X using lateral susceptibility distribution.

Figure 26: Three dimensional view for inverted depth to basement.

Figure 27: Inverted depth to basement surface from 3D magnetic modeling using constant susceptibility.

Figure 28: Inverted Vs. actual depths at drilled well location WKO-1X and WKO-3X using constant susceptibility.

Figure 29: Relationship between the root mean square value between inverted and actual depth on y-axis and the Dc initial depth to basement on x-axis.

Figure 30: Relationship between DC mean D.T.B on x-axis and the minimum error misfit between the observed and calculated data on y-axis.

Figure 31: relationship between DC mean D.T.B on x-axis and the mean error misfit between the observed and calculated data on y-axis.

Figure 32: relationship between DC mean D.T.B on x-axis and the maximum error misfit between the observed and calculated data on y-axis.

LIST OF TABLES

Table 1: Resolutions and Sampling Rates of the, Data Acquisition System.

Table 2: Values of FOM and Heading Calibration Flights

Table 3: Structural Indices for simple magnetic and gravity models used for depth estimations by Euler Deconvolution. The number of infinite dimensions describes the extension of the geologic model in space.

CHAPTER 1

INTRODUCTION

1.1. GENERAL

Aeromagnetic maps reflect spatially-varied anomalies of the earth magnetic field. These magnetic field variations are usually related to the distribution of subsurface magnetic susceptibility structures and/or remnant magnetization. Shallow-seated sedimentary rocks, in general, have low magnetic content compared with the deep-seated basement (igneous and metamorphic) rocks which tend to have a much greater magnetic content. Conventional semi-quantitative interpretational techniques, like local power spectra and analytical signal methods which are roughly used to estimate an averaged depth-to-the-basement and, indirectly, thickness of the sedimentary basin, can delineate such subsurface structures briefly. Alternatively, multi-dimensional inverse modeling (inversion) represents the up-to-date quantitative interpretational technique that can physically delineate both subsurface magnetic susceptibility structures and depth-to-the-basement from the observed aeromagnetic data either in spatial- or frequency-domain.

In applied aeromagnetics, the total magnetic intensity (TMI) data are measured as a result of the earth magnetic field. This is what we might call a 'forward problem'; a model is given and the data are calculated. The forward (direct) problem is always uniquely solvable. It is often the other way around; data have been measured and we wish to derive a reliable layered-earth model that is consistent with the data, what may be described as 'inverse problem' which is concerned with the problem of making magnetic susceptibility interfaces (layer boundaries) from the measured data. Since nearly all field data are subjected to some uncertainty, these interfaces are statistically dependent, and therefore no inverse problem in aeromagnetics is uniquely solvable, Due to such an invariable non-

linearity between the measured data and desired model parameters (layer susceptibility and thicknesses), we usually use an iterative procedure in which the non-linear inverse problem is replaced, at each iteration, by its linearized approximation to be solved. Throughout, the data and model parameter vectors are related via a non-linear response function, which tells us how to calculate the synthetic data from the given model. The overall goal of the inversion is then to minimize the deviation between the measured and calculated data, what may be described as the 'objective function.' To derive an iterative inversion scheme, the response function is linearized about a starting model (initial guess) by expanding it into a Taylor's series approximation and ignoring the higher terms. This is the classical 'Gauss–Newton' solution (Marquardt, 1963; Lines and Treitel, 1984; Webring 1985) which can be applied successively to improve (refine) the initial model until an optimal model update is obtained in an appropriate least-squares fashion. The process iterates until a given convergence criterion or a maximum number of iterations is reached. To determine how well the model fits the measured data, the usual weighted least-squares criterion (χ^2 or root mean-square (RMS) misfit) is used, attempting generally at minimizing the familiar estimate.

This full non-linear least-squares optimization algorithms, like layered-earth inversion schemes, try to solve an over-determined geophysical inverse problem (i.e. when model parameters are far less than collected data points), and hence requires a starting model which has the desired (not more) number of layers. It modifies (adjusts) the layer susceptibility and thicknesses in the starting model iteratively to best fit the data at some tolerance, allowing incorporating a-priori information to constrain the solution a bit (Marquardt, 1963). The Layered-earth inversion was carried out for RTP data in frequency-domain.

Once the magnetic survey is complete, the data are processed, and regional field is removed appropriately. The problem is conceptually

straightforward: Estimate some parameters of the source from observed magnetic fields, while incorporating all available geological, geophysical, and other independent related information. The stages of interpretation can be categorized into three categories (Figure 1). Each category has the same goal, to illuminate the distribution of magnetic sources, but they approach the same goal with quite different logical processes.

Forward method: a starting model is established depending on geologic and geophysical resources. The model's anomaly is calculated and correlated with the observed anomaly, and model parameters are modified to improve the fit between the two anomalies. This steps of body adjustment, anomaly calculation, and anomaly comparison is iterated until calculated and observed anomalies are sufficiently alike.

Inverse method: some parameters are calculated automatically and directly from the observed anomaly. Simplifying assumptions are inevitable (Blakely, R.J., 1995).

Data enhancement and display: No model parameters are calculated, while the anomaly is processed to improve specific properties of the source, as to make it easier for the interpretation. All available geologic and tectonic setting should be included in each process. Potential field studies, previous seismic refraction or reflection surveys, may be available to guide the modeling. The interpretation in any case will be originally not unique, but involving of independent information can minimize the infinite set of solutions to a controllable array of models, infinite in number but more geologically logical. It may seem from the previous description that the inverse method is considerably simpler and more straightforward than the forward method. (Blakely, R.J., 1995)

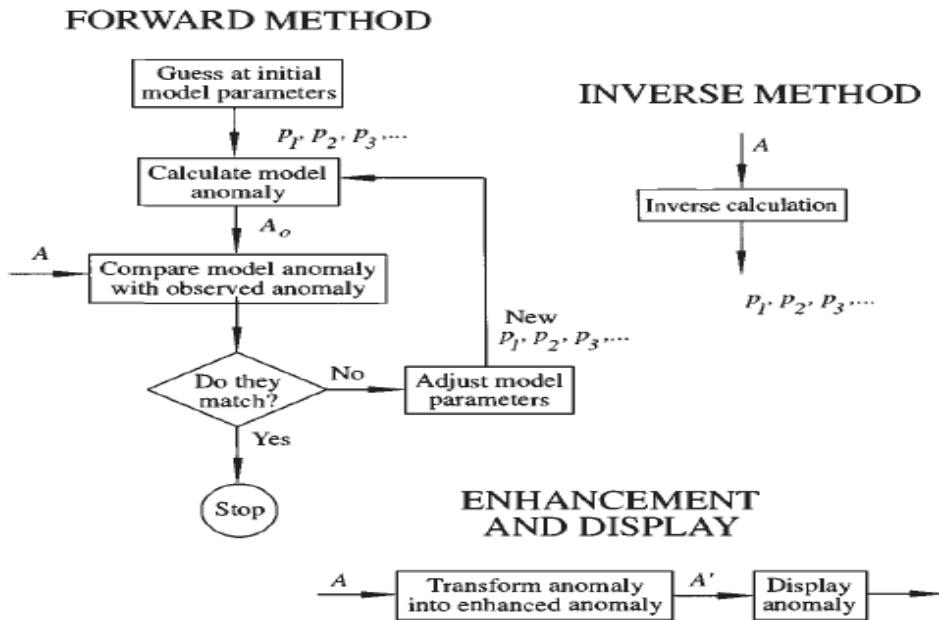


Figure 1: Three categories of techniques to interpret potential field data. Measured anomaly is represented by A , calculated anomaly by A_o , and transformed measured anomaly by A' . Parameters p_1, p_2, \dots are attributes of the source, such as depth, thickness, density, or magnetization.

1.2. LOCATION OF STUDY AREA

The present study area (West Edfu) area is located in the southern part of the Western Desert of Egypt, between Latitudes $24^{\circ}13'14''$ N & $26^{\circ}01'2''$ N and Longitudes $31^{\circ}06'$ E & $32^{\circ}42'43''$ E (Figure 2).